

# PHYSICAL PROPERTIES OF THE GAMMA-RAY BINARY LS 5039 THROUGH LOW AND HIGH FREQUENCY RADIO OBSERVATIONS

**Benito Marcote**

M. Ribó, J. M. Paredes, C. H. Ishwara-Chandra

HEPRO V

October 7, 2015



**B** Universitat de Barcelona



Institut de Ciències del Cosmos

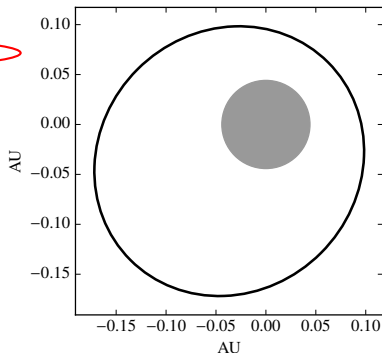
# Gamma-Ray Binaries

**Gamma-ray binaries:** binary systems which host a compact object orbiting a high mass star that have the non-thermal maximum of the Spectral Energy Distribution in  $\gamma$ -rays (Paredes et al. 2013, Dubus 2013).

System	Main star	$P$ / days
LS 5039	O6.5 V	3.9
1FGL J1018.6-5856	O6 V	16.6
LS I +61 303	B0 Ve	26.5
HESS J0632+057	B0 Vpe	315.0
PSR B1259-63	O9.5 Ve	1236.7
Cygnus X-3	WR	0.2
Cygnus X-1 ??	O9.7 Ve	5.6
MWC 656 ??	Be	60.4

Red: known gamma-ray binaries

Green: X-ray binaries with gamma-ray emission



# The gamma-ray binary LS 5039

$$\alpha_{J2000} = 18^{\text{h}} 26^{\text{m}} 15.06^{\text{s}}$$

$$\delta_{J2000} = -14^{\circ} 50' 54.3''$$

O6.5 V main-sequence star ( $23 \pm 3 M_{\odot}$ )  
Compact object, NS or BH ( $1-5 M_{\odot}$ )

$$P \approx 3.9 \text{ d}$$

$$e = 0.35 \pm 0.04$$

$$d = 2.5 \pm 0.5 \text{ kpc}$$

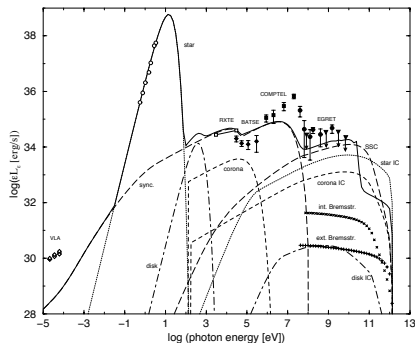
**X-rays:** periodic

**GeV light-curve:** periodic (anticorrelated)

**TeV light-curve:** periodic

**Radio:** persistent, small variability  
without orbital modulation

Aharonian et al. (2005), Casares et al. (2005), Kishishita et al. (2009), Abdo et al. (2009), Casares et al. (2012), Zabalza et al. (2013), Collmar & Zhang (2014)



SED of LS 5039 (Paredes et al. 2005)

# The gamma-ray binary LS 5039

$$\alpha_{J2000} = 18^{\text{h}} 26^{\text{m}} 15.06^{\text{s}}$$

$$\delta_{J2000} = -14^{\circ} 50' 54.3''$$

O6.5 V main-sequence star ( $23 \pm 3 M_{\odot}$ )

Compact object, NS or BH ( $1\text{--}5 M_{\odot}$ )

$$P \approx 3.9 \text{ d}$$

$$e = 0.35 \pm 0.04$$

$$d = 2.5 \pm 0.5 \text{ kpc}$$

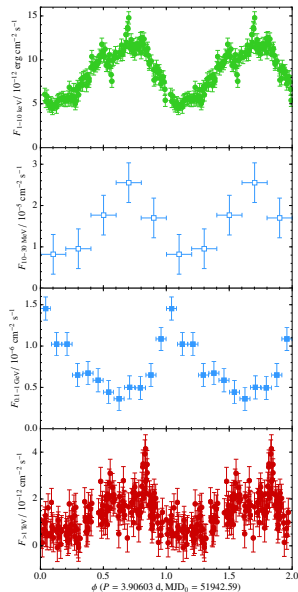
**X-rays:** periodic

**GeV light-curve:** periodic (anticorrelated)

**TeV light-curve:** periodic

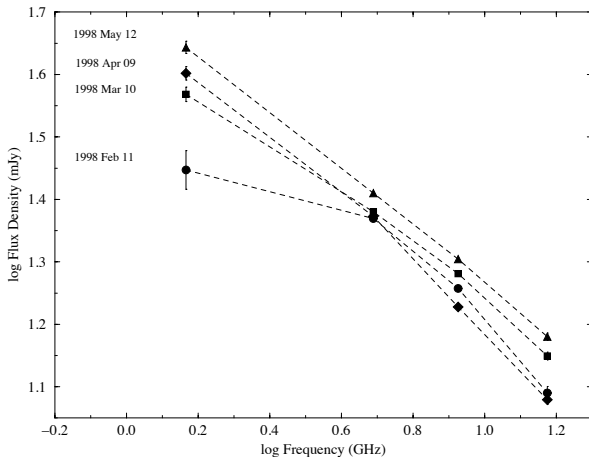
**Radio:** persistent, small variability  
without orbital modulation

Aharonian et al. (2005), Casares et al. (2005), Kishishita et al. (2009), Abdo et al. (2009), Casares et al. (2012), Zabalza et al. (2013), Collmar & Zhang (2014)



# Previous radio observations of LS 5039

- Variability from Martí et al. (1998)



Spectral index  $\alpha = -0.46 \pm 0.01$ , variability  $< \pm 25\%$

# Understanding the emission of Gamma-Ray Binaries

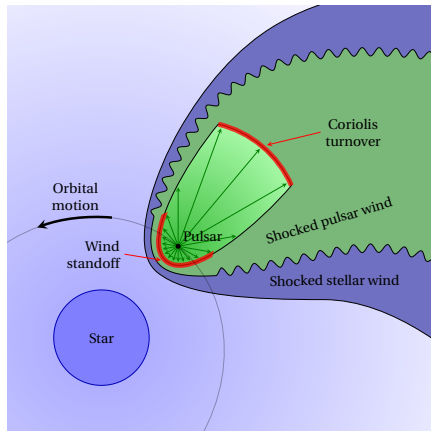
Young non-accreting pulsar scenario

Strong shock between both winds:

- Relativistic pair plasma wind from the pulsar
- Stellar wind from the massive companion star

Originally proposed by Maraschi & Treves (1981), re-proposed by Dubus (2006)

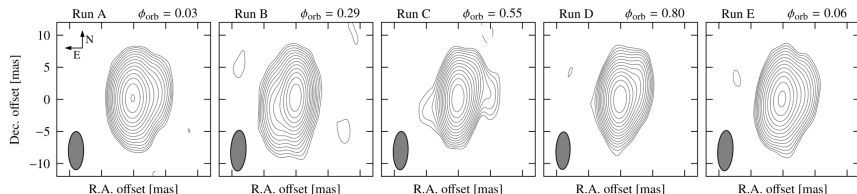
- **High energy** emission produced by synchrotron and inverse Compton.
- **Radio flux** dominated by the synchrotron emission (Bosch-Ramon 2009)



Model for LS 5039 (Zabalza et al. 2012)

# Previous radio observations of LS 5039

- VLBI observations: Moldón et al. (2012)



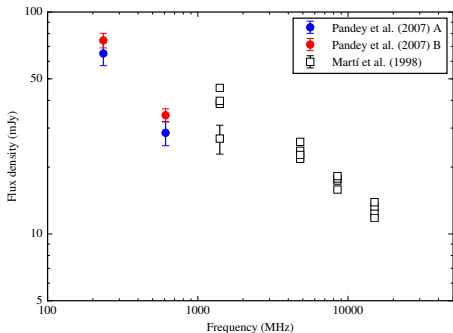
Observations along one orbital period.

Dominant core emission ( $\lesssim 1$  mas, or 3 AU).

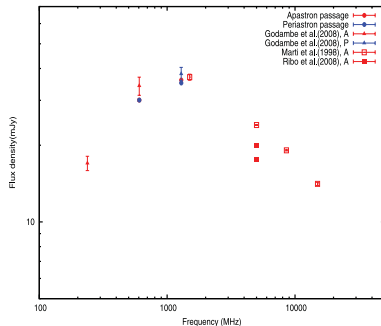
Extended emission orbitally modulated at mas scales ( $< 10\%$  of the total flux density emission).

# Previous radio observations of LS 5039

- At low frequencies, only a few observations have been published with contradictory results.



Adapted from Pandey et al. (2007)



Bhattacharyya et al. (2012)  
Godambe et al. (2008)

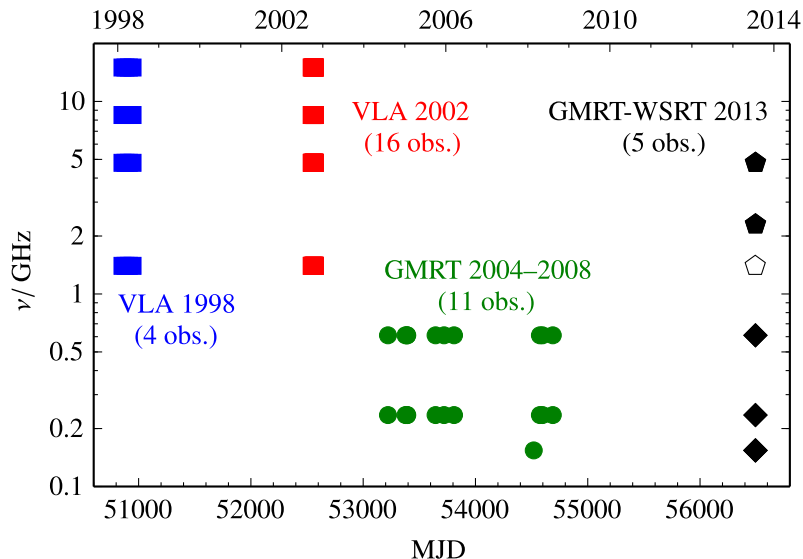
# Radio observations

Work published in Marcote et al. (2015)

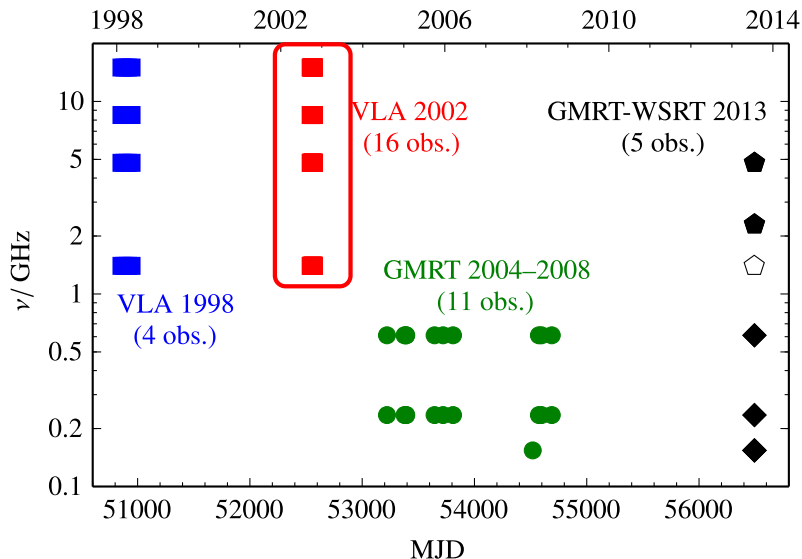
- 1.4–15 GHz (VLA)  
Monitoring in 1998, 2002
- 154, 235 & 610 MHz (GMRT)  
Archival observations 2004–08
- 154 MHz–5 GHz (GMRT & WSRT)  
Two quasi-simultaneous observations  
in 2013.



# Summary of the observations analyzed in this work

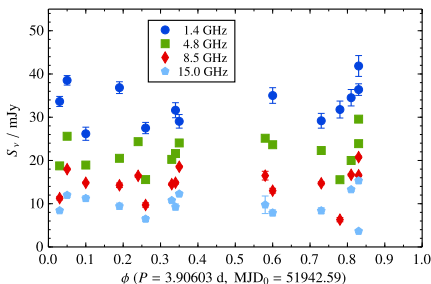
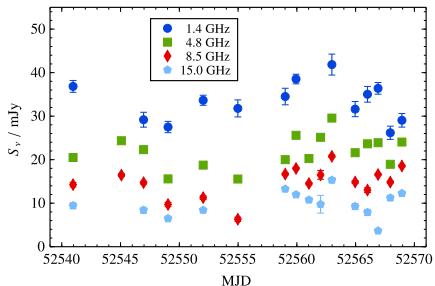


# Summary of the observations analyzed in this work



# High-frequency variability along the orbit

VLA monitoring in 2002



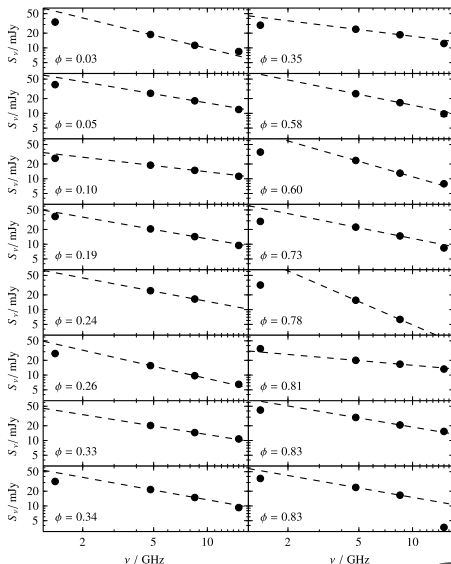
- Persistent flux density emission.
- Variability on timescales as short as one day.
- Variability  $< \pm 25\%$
- No visible orbital modulation

Flux density values at all frequencies compatible with the ones reported at other epochs (e.g. Martí et al. 1998).

# High-frequency variability along the orbit

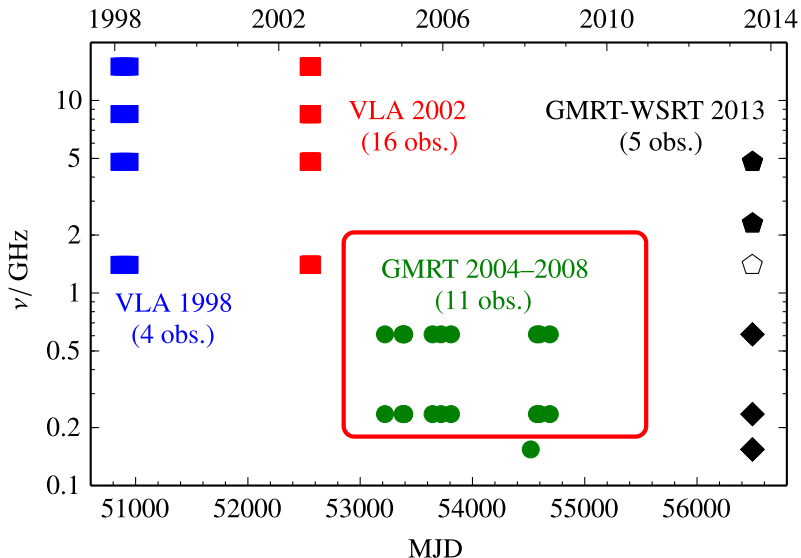
VLA monitoring in 2002

- Dashed lines represent the power-laws determined from 5.0 and 8.5 GHz
- We observe a  $\approx$  power-law at these GHz frequencies most of the times
- Slight curvature below 2 GHz
- Average spectral index:  
 $\alpha = -0.57 \pm 0.12$



# Low-frequency variability along the orbit

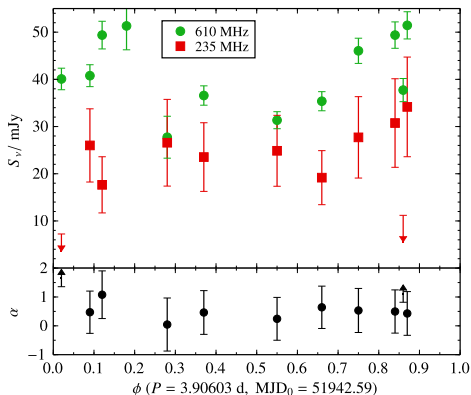
Archival GMRT observations 2004–2008



# Low-frequency variability along the orbit

Archival GMRT observations 2004–2008

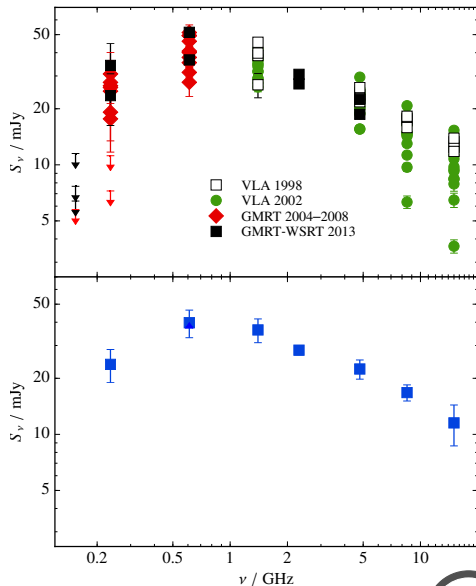
- Observations spread over 4 yr
- Persistent emission
- Variability at  $> 6\sigma$
- Average spectral index  
 $\alpha = +0.5 \pm 0.8$
- Hints of orbital modulation?



# Non-simultaneous spectrum of LS 5039

Combining data from 1998 to 2013

- Small variability along the years ( $< 25\% \quad \forall \nu$ )
  - “Similar” profile in average
  - Turnover at  $\sim 0.5$  GHz
  - Source undetected at 150 MHz
- 
- Only two data at 2.3 GHz (no statistics)
  - The mean square errors have been used in the average data



# Modeling the LS 5039 spectrum

A first approximation (toy model)

From VLBI observations (Moldón et al. 2012) we know that most of the radio emission comes from a compact core  $\lesssim 1$  mas ( $\sim 3$  AU) to be compared with the 0.19 AU of the semi major axis.

We have built a very simple model to understand the spectrum:

- Compact core  $\rightsquigarrow$  **one-zone model**
- No orbital modulation  $\rightsquigarrow$  **symmetric emitting region (spheric)**
- For simplicity  $\rightsquigarrow$  **isotropic and homogeneous**
- We consider the presence of a synchrotron emitting plasma
- Turnover produced either by SSA, FFA or Razin effect (and combinations of them)

# Modeling the LS 5039 spectrum

A first approximation (toy model)

We have built a very simple model to understand the spectrum:

- Synchrotron emission, with a particle injection:

$$n(E)dE = KE^{-p}dE$$

- Synchrotron self-absorption (SSA):

$$\kappa_{\text{SSA}} \propto KB^{(p+2)/2}\nu^{-(p+4)/2}$$

- Free-free absorption (FFA):

$$\kappa_{\text{FFA}} \propto n_e^2 T_w^{-3/2} \nu^{-2}$$

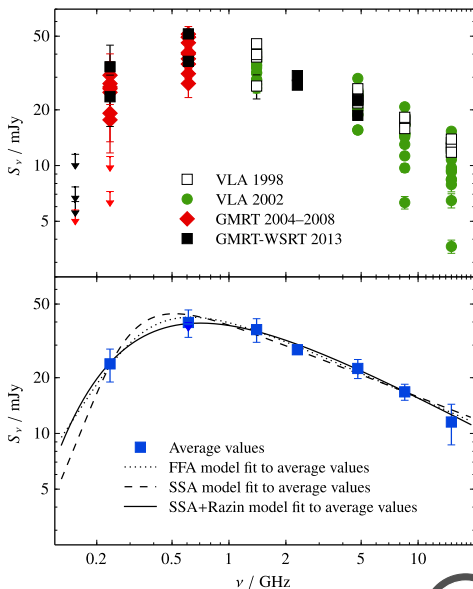
- Razin effect:

$$S_\nu \rightsquigarrow S_\nu e^{-\nu_R/\nu}, \quad \nu_R \equiv 20n_e B^{-1}$$

# Non-simultaneous spectrum of LS 5039

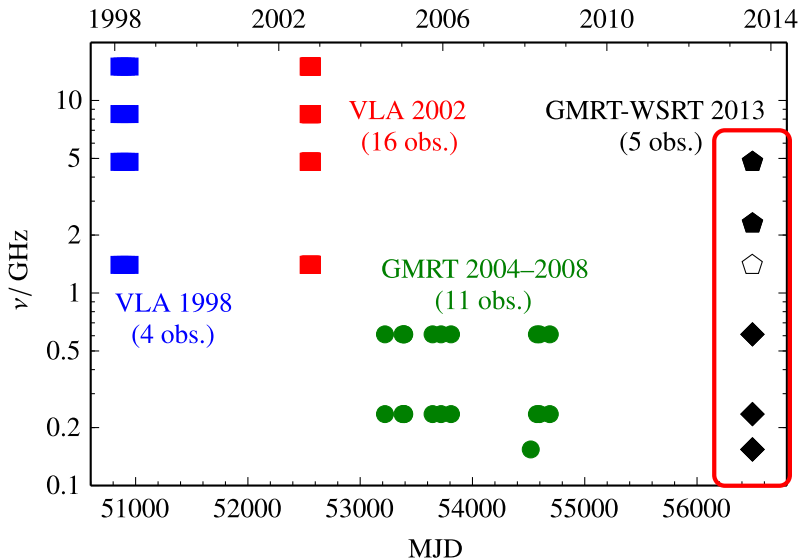
Combining data from 1998 to 2013

- The average spectrum can be fitted by typical models:
  - SSA
  - Synchrotron + FFA
  - SSA + Razin
  - FFA + Razin
  - SSA + FFA
- SSA+Razin effect is the best fit to the data
- But the other fits are not statistically rejected
- Small differences between all of them



# Quasi-simultaneous spectrum of LS 5039

GMRT & WSRT campaign in 2013 July 19 and 21

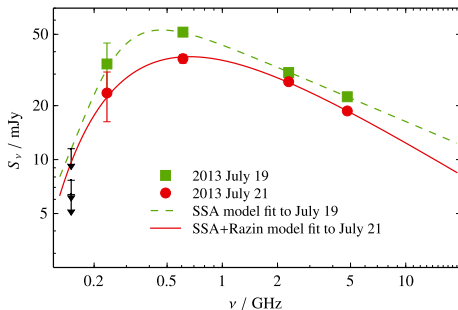


# Quasi-simultaneous spectrum of LS 5039

GMRT & WSRT campaign in 2013 July 19 and 21

Two 0.15–5 GHz spectra at orbital phases  $\phi \approx 0.9$  and 0.4.

- Although similar to the average spectrum, we observe subtle differences between the two epochs.
- The turnover at  $\sim 0.5$  GHz is persistent.
- Stronger emission on 2013 July 19.
- 2013 July 19: pure SSA spec.
- 2013 July 21: SSA+Razin spec.
- FFA provides poor fits



GMRT data: 235 and 610 MHz

WSRT data: 2.3 and 5.0 GHz

154 MHz GMRT data taken every other day  
(on 2013 July 18, 20 and 22)

# Modeling the LS 5039 spectrum

The three spectra show a similar shape but with subtle differences:

- Avg. spectrum: SSA+Razin
- July 19 spectrum: SSA
- July 21 spectrum: SSA+Razin

Fit	$\rho$	$\Omega B^{-1/2}$ [ $10^{-16} \text{ G}^{-1/2}$ ]	$K\ell B^{(p+2)/2}$ [ $10^3 \text{ cm G}^{(p+2)/2}$ ]	$\nu_R$ [ $10^8 \text{ Hz}$ ]
Avg. spectrum	$2.16 \pm 0.04$	$500 \pm 800$	$3 \pm 5$	$4.1 \pm 0.2$
July 19	$1.867 \pm 0.014$	$3.9 \pm 0.3$	$(2.1 \pm 0.9) \times 10^6$	–
July 21	$2.24 \pm 0.08$	$200 \pm 600$	$0.4 \pm 1.7$	$4.1 \pm 0.7$

- We can also compare these results with the free-free opacity inferred from the stellar wind (the region must be optically thin to FFA)

# Modeling the LS 5039 spectrum

Building a coherent picture from the fits and the free-free opacity:

- Avg. spectrum: SSA+Razin
- July 19 spectrum: SSA
- July 21 spectrum: SSA+Razin
- Coherent picture with:

$$\ell \sim 0.85 \text{ mas } (\sim 2.5 \text{ AU})$$

$$B \sim 20 \text{ mG}$$

$$n_e \sim 4 \times 10^5 \text{ cm}^{-3}$$

$$\dot{M} \sim 5 \times 10^{-8} M_{\odot} \text{ yr}^{-1}$$

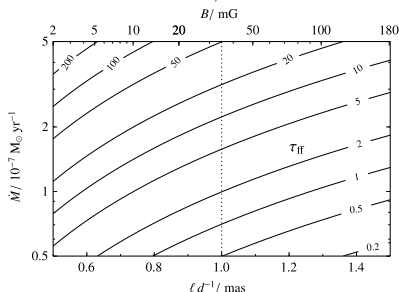
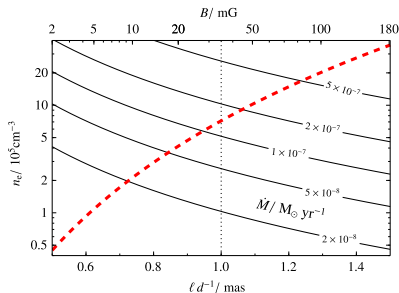
where:

$\ell$ : linear size of the emitting region,

$B$ : module of the magnetic field,

$n_e$ : electron density of the non-relativistic plasma,

$\dot{M}$ : mass-loss rate of the companion star.



# Modeling the LS 5039 spectrum

Building a coherent picture from the fits and the free-free opacity:

- Avg. spectrum: SSA+Razin
- July 19 spectrum: SSA
- July 21 spectrum: SSA+Razin
- Coherent picture with:

$$\ell \sim 0.85 \text{ mas } (\sim 2.5 \text{ AU})$$

$$B \sim 20 \text{ mG}$$

$$n_e \sim 4 \times 10^5 \text{ cm}^{-3}$$

$$\dot{M} \sim 5 \times 10^{-8} M_{\odot} \text{ yr}^{-1}$$

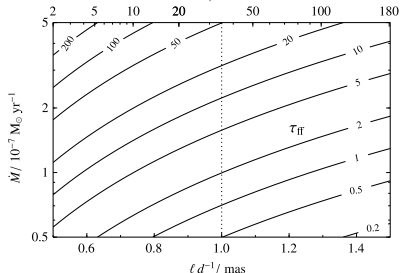
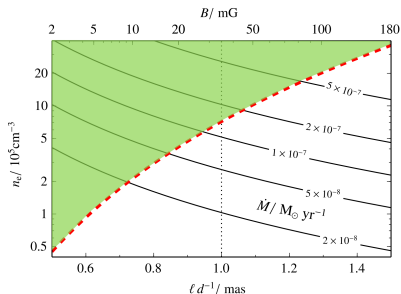
where:

$\ell$ : linear size of the emitting region,

$B$ : module of the magnetic field,

$n_e$ : electron density of the non-relativistic plasma,

$\dot{M}$ : mass-loss rate of the companion star.



# Modeling the LS 5039 spectrum

Building a coherent picture from the fits and the free-free opacity:

- Avg. spectrum: SSA+Razin
- July 19 spectrum: SSA
- July 21 spectrum: SSA+Razin
- Coherent picture with:

$$\ell \sim 0.85 \text{ mas } (\sim 2.5 \text{ AU})$$

$$B \sim 20 \text{ mG}$$

$$n_e \sim 4 \times 10^5 \text{ cm}^{-3}$$

$$\dot{M} \sim 5 \times 10^{-8} M_{\odot} \text{ yr}^{-1}$$

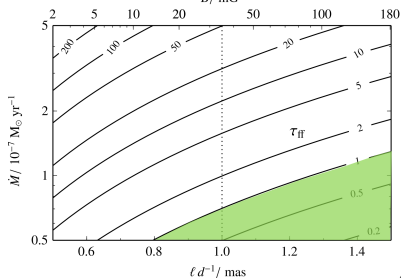
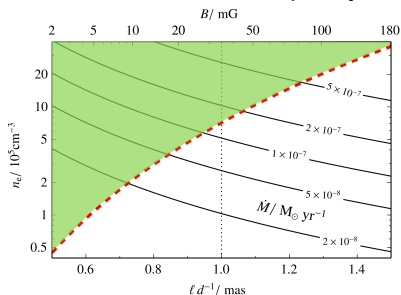
where:

$\ell$ : linear size of the emitting region,

$B$ : module of the magnetic field,

$n_e$ : electron density of the non-relativistic plasma,

$\dot{M}$ : mass-loss rate of the companion star.



# Modeling the LS 5039 spectrum

Building a coherent picture from the fits and the free-free opacity:

- Avg. spectrum: SSA+Razin
- July 19 spectrum: SSA
- July 21 spectrum: SSA+Razin
- Coherent picture with:

$$\ell \sim 0.85 \text{ mas } (\sim 2.5 \text{ AU})$$

$$B \sim 20 \text{ mG}$$

$$n_e \sim 4 \times 10^5 \text{ cm}^{-3}$$

$$\dot{M} \sim 5 \times 10^{-8} M_{\odot} \text{ yr}^{-1}$$

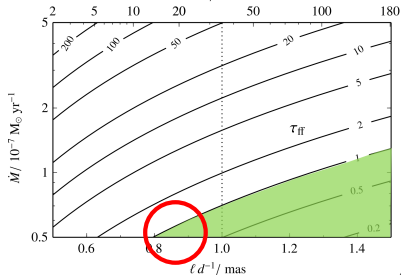
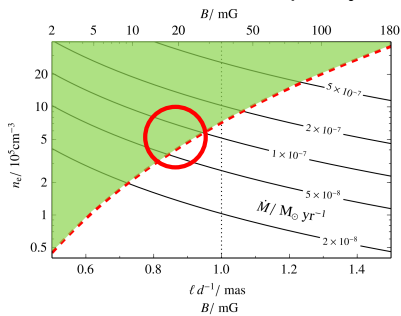
where:

$\ell$ : linear size of the emitting region,

$B$ : module of the magnetic field,

$n_e$ : electron density of the non-relativistic plasma,

$\dot{M}$ : mass-loss rate of the companion star.



# Modeling the LS 5039 spectrum

- A **significant mixing** of the non-relativistic wind inside the synchrotron radio emitting relativistic plasma, even close to  $\sim 100\%$ , is observed.
- The derived mass-loss rate (model dependent, in agreement with the last results, Casares, in prep.) implies that the wind is clumpy.
- The presence of Razin effect, widely observed in Colliding Wind Binaries, could give further support to the scenario of the young non-accreting pulsar.

# Conclusions

Marcote et al. (2015), MNRAS, 451, 59

Marcote (2015), PhD Thesis, Universitat de Barcelona

- We report day to day variability, trends on week timescales, and the absence of orbital variability. Variability  $< \pm 25\%$  is observed at all frequencies (0.23–15 GHz) even on year timescales.
- Persistent turnover at around  $\sim 0.5$  GHz.
- No detection up to now at 150 MHz
- The considered simple model can explain the observed spectra, indicating that the turnover is dominated by SSA
- A contribution of Razin effect is also observed at some epochs.
- Even with this simple model we have obtained a coherent picture that explains the observed spectra.
- Future multifrequency campaigns with more accurate results (specially at low frequencies) are required to compare with more detailed models.

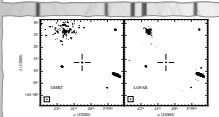
# Thank You...!

...and see also the poster about similar studies conducted for the gamma-ray binary LS I +61 303 (no. 20)!

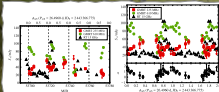
## Orbital and superorbital variability of LS I +61 303 at low radio frequencies with GMRT and LOFAR

B. Marcote<sup>1</sup>, M. Ribá, J. M. Paredes, C.H. Ishwara-Chandra, J. D. Swinbank, J. W. Brerick, S. Markoff, R. Fender, R. A. M. J. Wijers, C. C. Pauling, A. J. Stewart, M. E. Bell, R. P. Breton, D. Carbone, S. Corbel, J. Eisklauff, H. Falcke, J.-M. Grieblmeier, M. Kunigoshi, M. Pietka, A. Ronlinson, M. Serylak, A. J. van der Horst, J. van Leeuwen, M. W. Wise, P. Zarka  
<sup>1</sup>Departament d'Astronomia i Meteorologia, Institut de Ciències del Cosmos (ICCUB), Universitat de Barcelona (EEC-UB)

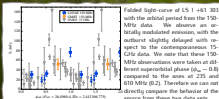
LS I +61 303 is a gamma-ray binary that exhibits an outburst at GHz frequencies each orbital cycle of 28.5 d and a superorbital modulation with a period of 48 yr. We have performed a detailed study of the low-frequency radio emission of LS I +61 303 by analyzing all the archival GMRT data at 150, 235 and 610 MHz, and conducting regular LOFAR observations within the Radio Sky Mapper (RSM) at 150 MHz. We have detected the source for the first time at 150 MHz, which is also the first detection of a gamma-ray binary at such a low frequency. We have obtained the light-curves of the source at 150, 235 and 610 MHz, all of them showing orbital modulation. The light-curves at 235 and 610 MHz also show the existence of superorbital variability. A comparison with contemporaneous 15-GHz data shows remarkable differences with these light-curves. As 15 GHz we see clear outbursts, whereas at low frequencies we see variability with wide maxima. The light-curve at 235 MHz seems to be anticorrelated with the one at 610 MHz, implying a shift of  $\sim 0.5$  orbital phases in the maxima. We model the shifts between the maxima at different frequencies as due to changes in the physical parameters of the emitting region assuming either free-free absorption or synchrotron self-absorption, obtaining expansion velocities for this region close to the stellar wind velocity with both mechanisms. The inferred values would give further support to the young non-accreting pulsar wind scenario. All these results are published in Marcote et al. (2015, submitted).



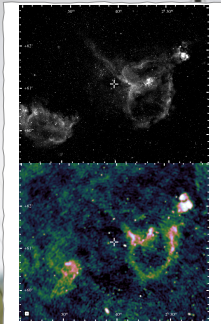
Detection of LS I +61 303 in the 2008 Feb 18 15A-MHz GMRT observation (left) and in the 2013 July 14 149-MHz LOFAR observation after removing baselines (right; 0.2 Jy inset).



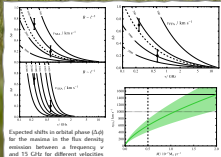
Flux density versus MJD (left) and orbital phase (right) for the archival GMRT and RT data. The black data (left bottom) shows the spectral index in the range of 235-610 MHz. We observe an orbital modulated light-curve. The 610-MHz data shows a quasi-sinusoidal modulation with a slower decay with respect to the 15-GHz data. The 235-MHz light-curve is almost anticorrelated with the one observed at 610 MHz.



Folded light-curve of LS I +61 303 with the orbital period from the 150-MHz data. We observe an orbitally modulated emission, with the outburst slightly delayed with respect to the contemporaneous 15-GHz data. We note that these 150-MHz observations were taken at different superorbital phases ( $\phi_{SO} = -0.8$ ) compared to the ones at 235 and 610 MHz ( $\phi_{SO} = 0.2$ ). Therefore we can not directly compare the behavior of the source from these two data sets.



Field of LS I +61 303 seen by PONS 5 (left) at an optical red  $I$  band (top), and by LOFAR at 149 MHz on 2013 July 14 (bottom).



Expected shifts in orbital phase ( $\Delta\phi$ ) for the maxima in the flux density emission between a frequency  $\nu$  and 15 GHz for different velocities of expansion of the radio emitting region considering synchrotron self-absorption with different dependences of the magnetic field with the size of the emitting region (see top figure) or free-free absorption (see top right column).

Inferred expansion velocity, assuming FFA, as a function of the mass-loss rate. The vertical dashed line denotes the expected mass-loss rate. We compare the obtained velocities with the mean stellar wind velocity (solid line) and the expected velocity (dotted line).

# Back-up slides

## Accurate GMRT data reduction (Marcote et al. 2015, Appendix)

Analyzing the GMRT data we found the reasons of the differences between Pandey et al. (2007) and Godambe et al. (2008):

- At low frequencies, the contribution of the Galactic diffuse emission is quite high within the Galactic Plane.
- It must be removed to recover the right flux densities in the final image. Otherwise the flux densities will be underestimate.
- Usually done automatically in most telescopes. Not in the GMRT.
- Godambe et al. (2008) did not take into account this correction.
- Pandey et al. (2007) used the Haslam approximation (see Marcote et al. 2015), extrapolating the emission seen at 408 MHz.
- We have conducted dedicated non correlated observations with the GMRT to directly measure the Galactic contribution in the field of LS 5039 to properly substract it.
- We have seen significant differences in these two methods for the field of LS 5039 (compatible with the comparison in Sirothia 2009).

## Razin effect

The synchrotron emission propagates through a plasma, which presents a refractive index  $n$ . Always that  $n < 1$  the beaming effect is partially suppressed. Although at high frequencies the effect is negligible, at low frequencies (with  $\nu \ll \nu_p$ , where  $\nu_p$  is the plasma frequency) it suppresses the beaming effect since

$$n^2 = 1 - \left(\frac{\nu_p}{\nu}\right)^2$$

and the beaming effect goes as

$$\theta_b \approx \gamma^{-1} = \sqrt{1 - n^2\beta^2}$$

- Presence of a thermal plasma surrounding the emitting region.
- Attenuation of the synchrotron radiation at low frequencies.
- Widely reported in Colliding Wind Binaries, solar wind, ...
- A good approximation is an exponential attenuation at low frequencies (Dougherty et al. 2003):

$$S_\nu \propto S_\nu e^{-\nu_R/\nu}, \quad \nu_R \equiv 20n_e B^{-1}$$